World Scientific
www.worldscientific.com

Study of capillary transit time distribution in coherent hemodynamics spectroscopy

Angelo Sassaroli*, Jana Kainerstorfer and Sergio Fantini

Department of Biomedical Engineering, Tufts University
4 Colby Street, Medford, MA 02155, USA
angelo.sassaroli@tufts.edu

A recently proposed analytical hemodynamic model[1] [S. Fantini, *NeuroImage* **85**, 202–221 (2014)] is able to predict the changes of oxy, deoxy, and total hemoglobin concentrations (model outputs) given arbitrary changes in blood flow, blood volume, and rate of oxygen consumption (model inputs). One assumption of this model is that the capillary compartment is characterized by a single blood transit time. In this work, we have extended the original model by considering a distribution of capillary transit times and we have compared the outputs of both models (original and extended) for the case of sinusoidal input signals at different frequencies, which realizes the new technique of coherent hemodynamics spectroscopy (CHS). For the calculations with the original model, we have used the mean value of the distribution of capillary transit times considered in the extended model. We have found that, for distributions of capillary transit times having mean values around 1 s and a standard deviation less than about 45% of the mean value, the original and extended models yield the same CHS spectra (i.e., model outputs versus frequency of oscillation) within typical experimental errors. For wider capillary transit time distributions, the two models yield different CHS spectra. By assuming that Poiseuille's law is valid in the capillary compartment, we have related the distribution of capillary transit times to the distributions of capillary lengths and capillary speed of blood flow to calculate the average capillary and venous saturations. We have found that, for standard deviations of the capillary transit time distribution that are less than about 80% of the mean value, the average capillary saturation is always larger than the venous saturation. By contrast, the average capillary saturation may be less than the venous saturation for wider distributions of the capillary transit times.

Keywords: Coherent hemodynamics spectroscopy; hemodynamic model; near-infrared spectroscopy; capillary transit time; hemoglobin saturation.

*Corresponding author.

A. Sassaroli, J. Kainerstorfer & S. Fantini

1. Introduction

Several hemodynamic models proposed in the literature have tried to address the complex relationship between the dynamics of tissue oxygen consumption, blood flow, and blood volume with those of some macroscopically measured signals. These models have been particularly useful for the physiological interpretation of the blood oxygen level dependent (BOLD) signal measured in functional magnetic resonance imaging (fMRI; see for example a review by Buxton[2]) and the optical signals measured in near-infrared spectroscopy (NIRS).[3–9] Some of the more sophisticated models proposed in NIRS are characterized by complex systems of differential equations that can be solved only numerically.[4,5,8] Recently, a new hemodynamic analytical model has been proposed by Fantini.[1] The model has been developed for both time- and frequency-domain data and can predict the absolute values or the changes of oxy, deoxy, and total hemoglobin concentrations (outputs of the model) given changes in tissue oxygen consumption, blood flow, and blood volume (inputs of the model). In the frequency domain, phasors (i.e., complex numbers expressed in terms of modulus and phase) are associated with sinusoidally oscillating inputs and outputs. For example, in the brain the input phasors represent the normalized oscillations of cerebral blood volume, cerebral blood flow, and cerebral metabolic rate of oxygen [$\mathbf{cbv}(\omega)$, $\mathbf{cbf}(\omega)$, and $\mathbf{cmro_2}(\omega)$, respectively] while the output phasors represent the oscillations of oxy, deoxy, and total hemoglobin concentrations[1] [$\mathbf{O}(\omega)$, $\mathbf{D}(\omega)$, and $\mathbf{T}(\omega)$, respectively]. We named this method of inducing blood volume and flow oscillations (and therefore oxy and deoxy hemoglobin oscillations) in target organs at different frequencies as coherent hemodynamics spectroscopy (CHS). The oscillations can be induced by different methods such as paced breathing,[10] leg cuffs inflations,[11] tilt bed, etc. Since the absolute value of modulus and phase of the output phasors (which are measured) are often difficult to control,[10–12] in CHS we measure the spectra of phasor ratios: $\mathbf{D}(\omega)/\mathbf{O}(\omega)$ and $\mathbf{O}(\omega)/\mathbf{T}(\omega)$. The hemodynamic model depends on 14 physiological parameters, which include the capillary and venous blood transit times, the baseline partial blood volumes in the three vascular compartments, and others that are described in our recent publications.[1,12] However, in CHS (which is based on

measurements of phasor ratios) we have shown that the number of independent parameters reduces to six.[12] One of the assumptions of the model is that the capillary and venous transit times (two parameters used in CHS) are single-valued parameters characterizing the overall circulation in the capillary and venous compartments. In this work, we have studied the spectra obtained in CHS for the more realistic case of a distribution of capillary transit times, and we have compared the results to those of the original model. We have also investigated how the distribution of capillary transit times affects the average capillary and venous saturations.

2. Materials and Methods

2.1. *Original hemodynamic model: Single value of capillary transit time*

The original hemodynamic model that is used in CHS to study the cerebral microcirculation is characterized by the following analytic expressions[12]:

$$\mathbf{O}(\omega) = \mathrm{ctHb}[S^{(a)}\mathrm{CBV}_0^{(a)}\mathbf{cbv}^{(a)}(\omega)$$
$$+ S^{(v)}\mathrm{CBV}_0^{(v)}\mathbf{cbv}^{(v)}(\omega)]$$
$$+ \mathrm{ctHb}\left[\frac{\langle s^{(c)}\rangle}{s^{(v)}}(\langle S^{(c)}\rangle - S^{(v)})\mathcal{F}^{(c)}\mathrm{CBV}_0^{(c)}\right.$$
$$\times \mathcal{H}_{\mathrm{RC-LP}}^{(c)}(\omega) + (S^{(a)} - S^{(v)})$$
$$\left.\times \mathrm{CBV}_0^{(v)}\mathcal{H}_{G-\mathrm{LP}}^{(v)}(\omega)\right][\mathbf{cbf}(\omega) - \mathbf{cmro_2}(\boldsymbol{\omega})]$$

$$(1)$$

$$\mathbf{D}(\omega) = \mathrm{ctHb}[(1 - S^{(a)})\mathrm{CBV}_0^{(a)}\mathbf{cbv}^{(a)}(\omega)$$
$$+ (1 - S^{(v)})\mathrm{CBV}_0^{(v)}\mathbf{cbv}^{(v)}(\omega)]$$
$$- \mathrm{ctHb}\left[\frac{\langle s^{(c)}\rangle}{s^{(v)}}(\langle S^{(c)}\rangle - S^{(v)})\mathcal{F}^{(c)}\mathrm{CBV}_0^{(c)}\right.$$
$$\times \mathcal{H}_{\mathrm{RC-LP}}^{(c)}(\omega) + (S^{(a)} - S^{(v)})$$
$$\left.\times \mathrm{CBV}_0^{(v)}\mathcal{H}_{G-\mathrm{LP}}^{(v)}(\omega)\right]$$
$$\times [\mathbf{cbf}(\omega) - \mathbf{cmro_2}(\boldsymbol{\omega})] \qquad (2)$$

$$\mathbf{T}(\omega) = \mathrm{ctHb}[\mathrm{CBV}_0^{(a)}\mathbf{cbv}^{(a)}(\omega) + \mathrm{CBV}_0^{(v)}\mathbf{cbv}^{(v)}(\omega)],$$

$$(3)$$

where $\mathbf{O}(\omega)$, $\mathbf{D}(\omega)$, $\mathbf{T}(\omega)$ are the phasors that describe the oscillations of oxy, deoxy, and total hemoglobin concentrations (model outputs), and $\mathbf{cbv}(\omega)$, $\mathbf{cbf}(\omega)$, and $\mathbf{cmro_2}(\omega)$ are the phasors associated with the

oscillations of cerebral blood volume, blood flow, and metabolic rate of oxygen (model inputs), respectively; $\mathcal{H}_{\mathrm{RC-LP}}^{(c)}(\omega)$ and $\mathcal{H}_{G-\mathrm{LP}}^{(v)}(\omega)$ are the complex transfer functions associated with blood circulation in the capillary bed and in the venous compartment, respectively [defined below in Eqs. (4) and (5)]; ctHb is the hemoglobin concentration in blood, and $\mathcal{F}^{(c)}$ is the Fåhraeus factor (ratio of capillary-to-large vessel hematocrit); the superscripts (a), (c), and (v) indicate the arterial (a), capillary (c), and venous (v) compartment values of hemoglobin saturation (S), static blood volume (CBV_0) and oscillatory blood volume $(\mathbf{cbv})$. The oscillatory capillary blood volume $[\mathbf{cbv}^{(c)}(\omega)]$ was set to zero because of the negligible dynamic dilation and recruitment of capillaries in the brain.[13,14] The transfer functions for the capillary and venous compartments represent resistor–capacitor (RC) and Gaussian low-pass filters, respectively[1]:

$$\mathcal{H}_{\mathrm{RC-LP}}^{(c)}(\omega) = \frac{1}{1 + i\omega \frac{t^{(c)}}{e}}, \qquad (4)$$

$$\mathcal{H}_{G-\mathrm{LP}}^{(v)}(\omega) = e^{-\frac{\ln 2}{2}\left[\omega\left(\frac{t^{(c)}+t^{(v)}}{3.56}\right)\right]^2} e^{-i\omega\left(\frac{t^{(c)}+t^{(v)}}{2}\right)}. \qquad (5)$$

Equations (4) and (5) describe the low-pass filter effect of the capillary and venous compartments, which are considered as linear time-invariant systems having $\mathbf{cbf}(\omega)$ and $\mathbf{cmro_2}(\omega)$ as inputs, and the cerebral oxy and deoxyhemoglobin concentrations $[\mathbf{O}(\omega), \mathbf{D}(\omega)]$ as outputs. We note that the transfer functions depend on two singled-value parameters, the capillary transit time $(t^{(c)})$ and the venous transit time $(t^{(v)})$, which determine the characteristic time constants of the capillary and venous transfer functions. The key time constants, which represent the inverse of the low-pass cutoff angular frequency, are $\sim t^{(c)}/e$ for the capillary compartment and $\sim [t^{(c)}+t^{(v)}]/3.56$ for the venous compartment.[1]

According to this model, the average capillary saturation, $\langle S^{(c)}\rangle$, and the venous saturation, $S^{(v)}$, are related to the arterial saturation, $S^{(a)}$, by the following relationships:

$$\langle S^{(c)}\rangle = S^{(a)}\left(\frac{1 - e^{-\alpha t^{(c)}}}{\alpha t^{(c)}}\right), \qquad (6)$$

$$S^{(v)} = S^{(a)}e^{-\alpha t^{(c)}}, \qquad (7)$$

where α is the rate constant of oxygen diffusion from capillary blood (and from blood in the smaller arterioles) to tissue.

Because of the high-pass nature of the cerebral autoregulation process that regulates cerebral blood flow in response to blood pressure changes,[15,16] we introduce the following relationship between $\mathbf{cbf}$ and $\mathbf{cbv}$[1,12]:

$$\mathbf{cbf}(\omega) = k\,\mathcal{H}_{\mathrm{RC-HP}}^{(\mathrm{AR})}(\omega)\mathbf{cbv}(\omega) = k\,\mathcal{H}_{\mathrm{RC-HP}}^{(\mathrm{AR})}(\omega)$$
$$\times \left[\frac{\mathrm{CBV}_0^{(a)}}{\mathrm{CBV}_0}\mathbf{cbv}^{(a)}(\omega) + \frac{\mathrm{CBV}_0^{(v)}}{\mathrm{CBV}_0}\mathbf{cbv}^{(v)}(\omega)\right], \qquad (8)$$

where we consider blood volume as a surrogate for blood pressure, k is the inverse of the modified Grubb's exponent, and $\mathcal{H}_{\mathrm{RC-HP}}^{(\mathrm{AR})}(\omega)$ is the RC high-pass transfer function that describes cerebral autoregulation. $\mathcal{H}_{\mathrm{RC-HP}}^{(\mathrm{AR})}(\omega)$ is given by the following expression:

$$\mathcal{H}_{\mathrm{RC-HP}}^{(\mathrm{AR})}(\omega) = \frac{\omega}{\omega - i\omega_c^{(\mathrm{AR})}}, \qquad (9)$$

where $\omega_c^{(\mathrm{AR})}$ is the cutoff angular frequency for autoregulation.

2.2. *Extended hemodynamic model: Distribution of capillary transit times*

In our extension of the original model to the case of multiple capillary transit times (which we indicate here with $\tau = t^{(c)}$), we introduce a distribution of capillary transit times described by a gamma probability density function (pdf)[17] $h(\tau; \gamma, \beta)$:

$$h(\tau; \gamma, \beta) = \frac{\tau^{\gamma-1}e^{-\frac{\tau}{\beta}}}{\beta^\gamma\Gamma(\gamma)}, \qquad (10)$$

where γ (dimensionless) and β (units of time) are constants, and $\Gamma(\gamma)$ is the gamma function evaluated at γ. It can be shown that the mean, $\langle\tau\rangle$, and standard deviation, $\sigma(\tau)$, of the continuous random variable τ are given by $\langle\tau\rangle = \gamma\beta$ and $\sigma(\tau) = \beta\sqrt{\gamma}$. By using this pdf of the capillary transit times, we can redefine the phasors $\mathbf{O}(\omega)$, $\mathbf{D}(\omega)$, and $\mathbf{T}(\omega)$ as follows:

$$\mathbf{O}_{\mathrm{mCTT}}(h, \omega) = \int_0^\infty h(\tau; \gamma, \beta)\mathbf{O}(\tau, \omega)d\tau, \qquad (11)$$

$$\mathbf{D}_{\mathrm{mCTT}}(h, \omega) = \int_0^\infty h(\tau; \gamma, \beta)\mathbf{D}(\tau, \omega)d\tau, \qquad (12)$$

$$\mathbf{T}_{\mathrm{mCTT}}(h, \omega) = \mathbf{O}_{\mathrm{mCTT}}(\tau, \omega) + \mathbf{D}_{\mathrm{mCTT}}(\tau, \omega), \qquad (13)$$

where $\mathbf{O}(\tau, \omega)$ and $\mathbf{D}(\tau, \omega)$ are defined by Eqs. (1) and (2) for any given value of the capillary transit time τ, and the subscripts "mCTT" indicate the multiple capillary transit times that result in the integration of the phasors $\mathbf{O}(\tau, \omega)$ and $\mathbf{D}(\tau, \omega)$ over the entire range of transit times weighted by $h(\tau; \gamma, \beta)$.

For comparison with experimental data collected in CHS, we are interested in the phasor ratios[10–12]:

$$\frac{\mathbf{D}_{\mathrm{mCTT}}(\omega)}{\mathbf{O}_{\mathrm{mCTT}}(\omega)} = \frac{|\mathbf{D}_{\mathrm{mCTT}}(\omega)|}{|\mathbf{O}_{\mathrm{mCTT}}(\omega)|} \mathrm{e}^{i\{\mathrm{Arg}[\mathbf{D}_{\mathrm{mCTT}}(\omega)] - \mathrm{Arg}[\mathbf{O}_{\mathrm{mCTT}}(\omega)]\}},$$

(14)

$$\frac{\mathbf{O}_{\mathrm{mCTT}}(\omega)}{\mathbf{T}_{\mathrm{mCTT}}(\omega)} = \frac{|\mathbf{O}_{\mathrm{mCTT}}(\omega)|}{|\mathbf{T}_{\mathrm{mCTT}}(\omega)|} \mathrm{e}^{i\{\mathrm{Arg}[\mathbf{O}_{\mathrm{mCTT}}(\omega)] - \mathrm{Arg}[\mathbf{T}_{\mathrm{mCTT}}(\omega)]\}}.$$

(15)

Therefore, the following four quantities are calculated at each frequency ω: $|\mathbf{D}_{\mathrm{mCTT}}(\omega)|/|\mathbf{O}_{\mathrm{mCTT}}(\omega)|$, $\mathrm{Arg}[\mathbf{D}_{\mathrm{mCTT}}(\omega)] - \mathrm{Arg}[\mathbf{O}_{\mathrm{mCTT}}(\omega)]$, $|\mathbf{O}_{\mathrm{mCTT}}(\omega)|/|\mathbf{T}_{\mathrm{mCTT}}(\omega)|$, $\mathrm{Arg}[\mathbf{O}_{\mathrm{mCTT}}(\omega)] - \mathrm{Arg}[\mathbf{T}_{\mathrm{mCTT}}(\omega)]$. These four quantities are then compared with the corresponding four quantities obtained with the original model described in Sec. 2.1. For both models we have assumed that $\mathbf{cmro_2}(\omega) = 0$.

2.3. *Effects of capillary transit time distribution on the average capillary and venous saturations*

According to our hemodynamic model, the average capillary saturation for a capillary transit time τ is $\langle S^{(c)} \rangle(\tau) = S^{(a)}(1 - \mathrm{e}^{-\alpha\tau})/(\alpha\tau)$ [see Eq. (6)]. A specific capillary characterized by a blood transit time τ contributes to the saturation of a draining venule by an amount proportional to the saturation at the end of the capillary, which is $S^{(v)}(\tau) = S^{(a)}\mathrm{e}^{-\alpha\tau}$ [see Eq. (7)], and to its speed of blood flow. In other words, due to the law of flow conservation, the venous saturation results from a weighted average of the final saturation of the confluent capillaries, with weights given by the blood flow velocities in each capillary. On the contrary, the average capillary saturation results from a spatial average over the capillary lengths.

In order to derive the distribution of capillary lengths and blood flow velocities from the distribution of capillary transit times $[h(\tau; \gamma\beta)]$, we have assumed that Poiseuille's law is valid in the capillary

compartment[8]:

$$R = \frac{128\eta l}{\pi d^4},$$

(16)

where R is the resistance of a vessel of length l and diameter d, and η is the blood viscosity. We also assume a simple circuital equivalent relationship between capillary flow (F) in the capillary and pressure difference (ΔP) at the extremities of the capillary[8]:

$$\Delta P = RF,$$

(17)

where R is the resistance defined by Eq. (16). Since $F = \sigma^{(c)}c^{(c)}$, where $\sigma^{(c)}$ is the capillary cross section (assumed to be constant) and $c^{(c)}$ is the capillary flow velocity, from Eqs. (16) and (17) we deduce that $c^{(c)} \propto 1/l$ (assuming that ΔP is also constant). In each capillary, the transit time (τ), the flow velocity ($c^{(c)}$), and the length (l) are related by: $\tau = l/c^{(c)}$. Therefore we can write that: $l \propto \sqrt{\tau}$ and $c^{(c)} \propto 1/\sqrt{\tau}$. The capillary length l and the capillary flow velocity $c^{(c)}$ are functions of the random variable τ therefore they are also random variables. The pdf of $c^{(c)}$ satisfies: $f_{c^{(c)}} dc^{(c)} = h(\tau; \alpha, \beta)d\tau$, where $f_{c^{(c)}}$ and $dc^{(c)}$ are the pdf and the differential of $c^{(c)}$. Similarly the pdf of the capillary length satisfies: $f_l\, dl = h(\tau; \gamma, \beta)d\tau$ where f_l and dl are the pdf and the differential of l, respectively. Given the information provided above, we can finally write the expressions of the average capillary [Eq. (18)] and venous saturations [Eq. (19)]:

$$\langle S^{(c)} \rangle_{\mathrm{mCTT}} = \frac{\int_0^\infty \langle S^{(c)} \rangle(\tau) \sqrt{\tau} h(\tau; \gamma, \beta) d\tau}{\int_0^\infty \sqrt{\tau} h(\tau; \gamma, \beta) d\tau},$$

(18)

$$S^{(v)}_{\mathrm{mCTT}} = \frac{\int_0^\infty S^{(v)}(\tau) \frac{h(\tau; \gamma, \beta)}{\sqrt{\tau}} d\tau}{\int_0^\infty \frac{h(\tau; \gamma, \beta)}{\sqrt{\tau}} d\tau}.$$

(19)

We have compared the saturations given by Eqs. (18) and (19) with those provided by the original model [Eqs. (6) and (7)], where we set the single-value capillary transit time $t^{(c)} = \langle \tau \rangle$.

3. Results

The results presented in this section were obtained by solving numerically the integrals of Eqs. (11) and (12) and Eqs. (18) and (19), by choosing a time step of 1 ms. The calculations were carried out at seven oscillation frequencies that can be typically induced in

human subjects *in vivo* by cyclically varying the arterial blood pressure with a variety or protocols (paced breathing, periodic cuff occlusion, etc.). The seven frequencies considered were 1/40, 1/35, 1/30, 1/25, 1/20, 1/15, and 1/10 Hz. The parameters of the original model [Eqs. (1) and (2)] were set to the following values: $|\mathbf{cbv}^{(a)}(\omega)| = \mathbf{cbv}^{(v)}(\omega) = 0.02$, $\mathrm{Arg}[\mathbf{cbv}^{(a)}(\omega)] = \mathrm{Arg}[\mathbf{cbv}^{(v)}(\omega)] = 0$; $k = 5$, ctHB $= 2.3$ mM, $\mathrm{CBV}_0^{(a)} = \mathrm{CBV}_0^{(v)} = 0.005$, $\mathrm{CBV}_0^{(c)} = 0.015$, $\mathcal{F}^{(c)} = 0.8, \alpha = 0.8, S^{(a)} = 0.98, t^{(v)} = 3$ s, $\omega_c^{(\mathrm{AR})}/2\pi = 0.1$ Hz. These parameters were chosen according to data reported in the published literature.[18–22]

Figure 1(a) shows the pdf of the capillary transit time, $h(\tau; \gamma, \beta)$ for $\gamma = 5$ and $\beta = 0.2$ s, corresponding to $\langle \tau \rangle = 1$ s and $\sigma(\tau) \approx 0.45$ s (i.e., 45% of $\langle \tau \rangle$). We used the original and the extended models to compute the four quantities of interest in CHS: $|\mathbf{D}(\omega)|/|\mathbf{O}(\omega)|$, $\mathrm{Arg}[\mathbf{D}(\omega)] - \mathrm{Arg}[\mathbf{O}(\omega)]$, $|\mathbf{O}(\omega)|/|\mathbf{T}(\omega)|$, $\mathrm{Arg}[\mathbf{O}(\omega)] - \mathrm{Arg}[\mathbf{T}(\omega)]$ [see Fig. 1(b)]. In Fig. 1(b), the crosses were obtained with the original model (characterized by a single capillary transit time, which was chosen as $t^{(c)} = \langle \tau \rangle = 1$ s) and the empty circles were obtained with the extended model using the capillary time distribution of Fig. 1(a). The maximum discrepancy between the ratios of oscillation amplitudes (i.e., the ratio of phasors' modulus) calculated with the two models is about 4% ($|\mathbf{D}|/|\mathbf{O}|$) and 1% ($|\mathbf{O}|/|\mathbf{T}|$). As for the phase differences of phasors, the maximum

discrepancies were $\sim 1°$ for both $\mathrm{Arg}(\mathbf{D}) - \mathrm{Arg}(\mathbf{O})$ and $\mathrm{Arg}(\mathbf{O}) - \mathrm{Arg}(\mathbf{T})$. These discrepancies are of the same order of magnitude of typical experimental errors found in the measurements of these quantities. The average capillary and venous saturation values calculated with the extended model were $\langle S^{(c)} \rangle_{\mathrm{mCTT}} \approx 0.66$ and $\langle S^{(v)} \rangle_{\mathrm{mCTT}} \approx 0.50$, while the capillary and venous saturations calculated with the original model were $\langle S^{(c)} \rangle (t^{(c)} = \langle \tau \rangle) \approx 0.67$ and $\langle S^{(c)} \rangle (t^{(c)} = \langle \tau \rangle) \approx 0.44$.

Figure 2(a) shows the pdf of the capillary transit time, $h(\tau; \gamma, \beta)$ for $\gamma = 1.108$ and $\beta = 1.26$ s, corresponding to $\langle \tau \rangle \approx 1.4$ s and $\sigma(\tau) \approx 1.33$ s (i.e., 95% of $\langle \tau \rangle$). This is a wider distribution, having mean and standard deviation values that have been measured on a group of rats under resting conditions.[23] Although the distribution of transit times measured in the work of Stefanovic *et al.*[23] is not closely represented by a gamma distribution, here we continue considering a gamma distribution for the capillary transit times.[17] In Fig. 2(b), we show the CHS spectra obtained with the two models. The cross symbol is used for the original model whereas the empty circle is used for the extended model. The phase differences of phasors generated by the two models differ by less than $\sim 13°$ for $\mathrm{Arg}(\mathbf{D}) - \mathrm{Arg}(\mathbf{O})$ and less than $\sim 1.5°$ for $\mathrm{Arg}(\mathbf{O}) - \mathrm{Arg}(\mathbf{T})$. The ratio of oscillations amplitude (i.e., the modulus of phasors' ratio) generated
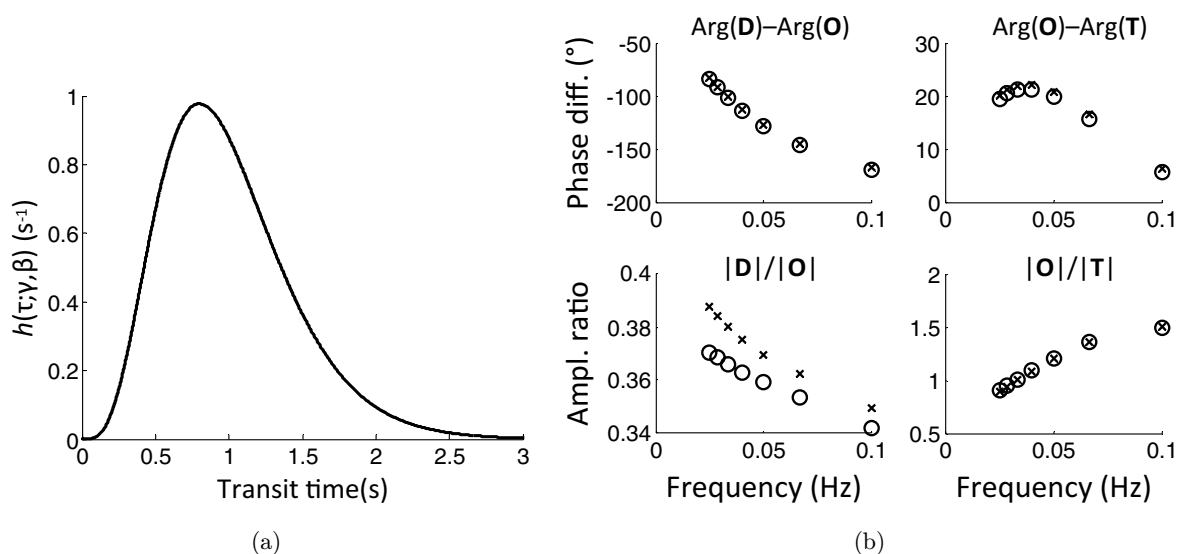

(a)   (b)

Fig. 1. (a) pdf of the capillary transit time $[h(\tau; \gamma, \beta)]$ for $\gamma = 5$ and $\beta = 0.2$ s, which yield $\langle \tau \rangle = 1$ s and $\sigma(\tau) \approx 0.45$ s. (b) CHS spectra of phase differences $[\mathrm{Arg}(\mathbf{D}) - \mathrm{Arg}(\mathbf{O})$ and $\mathrm{Arg}(\mathbf{O}) - \mathrm{Arg}(\mathbf{T})]$ and amplitude ratios $[|\mathbf{D}|/|\mathbf{O}|$ and $|\mathbf{O}|/|\mathbf{T}|]$ as a function of the oscillation frequency. The crosses represent data obtained with the original model, whereas the empty circles represent data obtained with the extended model.
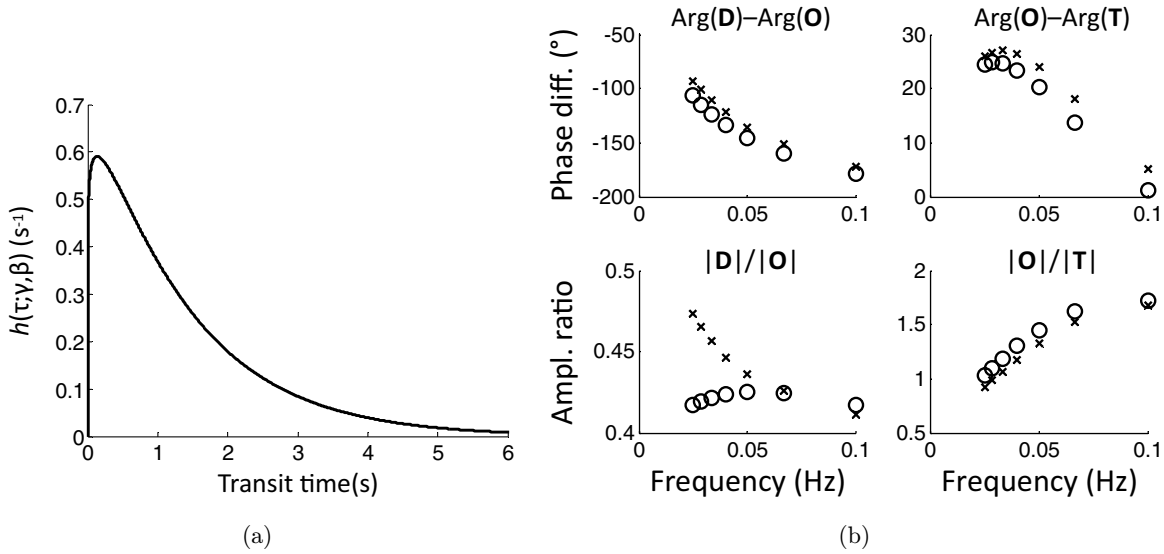
Fig. 2. (a) pdf of the capillary transit time $[h(\tau; \gamma, \beta)]$ for $\gamma = 1.108$ and $\beta = 1.26\,\mathrm{s}$, which yield $\langle\tau\rangle \approx 1.4\,\mathrm{s}$ and $\sigma(\tau) \approx 1.33\,\mathrm{s}$. (b) CHS spectra of phase differences $[\mathrm{Arg}(\mathbf{D})-\mathrm{Arg}(\mathbf{O})$ and $\mathrm{Arg}(\mathbf{O})-\mathrm{Arg}(\mathbf{T})]$ and amplitude ratios $[|\mathbf{D}|/|\mathbf{O}|$ and $|\mathbf{O}|/|\mathbf{T}|]$ as a function of the oscillation frequency. The crosses represent data obtained with the original model, whereas the empty circles represent data obtained with the extended model.

by the two models differ by less than $\sim 13\%$ for $|\mathbf{D}|/|\mathbf{O}|$ and less than $\sim 10\%$ for $|\mathbf{O}|/|\mathbf{T}|$. Note also that the spectral trends (i.e., the frequency dependence) of $|\mathbf{D}|/|\mathbf{O}|$ obtained by the two models are quite different. Therefore, we can state that for wider capillary transit time distributions (standard deviation approaching the mean value) the discrepancies between the two models are larger than typical errors found in the measurements of the quantities of interest in CHS.

Regarding the average capillary and venous saturation values for the original model (single capillary transit time) we obtained $\langle S^{(c)}\rangle(t^{(c)} = \langle\tau\rangle) \approx 0.59$ and $S^{(v)}(t^{(c)} = \langle\tau\rangle) \approx 0.32$. The extended model yielded $\langle S^{(c)}\rangle_{\mathrm{mCTT}} \approx 0.55$ and $S^{(v)}_{\mathrm{mCTT}} \approx 0.64$, i.e., an average capillary saturation that is lower than the venous saturation. We note that an average capillary saturation lower than the venous saturation has been recently measured in animal models.[24]

We have run calculations for different values of the parameters γ and β of the distribution function $h(\tau; \gamma, \beta)$ that are reported in Table 1 of the article by Jespersen and Østergaard[17] to represent measurements on rats during baseline and under various stimulations conditions. We can summarize our results by saying that for distributions of capillary transit times with $\sigma(\tau)/\langle\tau\rangle \lesssim 45\%$, the discrepancies between the spectra generated by the two models

are within the experimental errors. Furthermore, the calculations on the average capillary and venous saturations have shown that for distributions of capillary transit times having $\sigma(\tau)/\langle\tau\rangle \lesssim 80\%$ the average capillary saturation is always greater than the venous saturation. The opposite is true for wider distributions of capillary transit times.

4. Discussion

In this work, we have investigated the effect of a capillary transit time distribution on the spectra obtained with the novel technique of CHS and on the computed values of average capillary and venous saturations. We have defined new formulas that incorporate the capillary transit time distribution in the calculation of oxy and deoxy hemoglobin oscillations [Eqs. (11) and (12)]. The CHS spectra derived with this new extended model have been compared with those obtained with the original model based on a single capillary transit time. We have found that whenever distributions are relatively "narrow" (i.e., distributions having mean value and standard deviation such that $\sigma(\tau)/\langle\tau\rangle \leq 45\%$) the spectra obtained with the two models yield the same values to within experimental errors. For wider distributions, the two models yield increasingly different spectra.

We have also investigated the question of how the choice of baseline parameters affect the CHS

spectra (data not shown). In particular from our preliminary data, we have found that changing α, (up to 20% of the value assumed in this study) and the baseline blood volumes (up to three times of the values assumed in this study), has negligible effect on the spectra compared with the effect of the distribution of capillary transit times. In fact, we recall that CHS spectra are based on amplitude ratios and phase differences of oxy- and deoxy (or oxy and total) hemoglobin oscillations rather than on the absolute values of the oscillating hemoglobin species. Therefore, we argue that the choice of the baseline parameters has a lesser impact on the CHS spectra than on the computed amplitude and phase of the individual oscillations of the hemoglobin species.

We have also tested our model for the calculation of the oxygen extraction factor [defined as OEF = $(S^{(a)} - S^{(v)})/S^{(a)}$] in the two different situations addressed also by Jespersen and Østergaard[17]: (a) for a single transit time (taken to be the mean value of the distribution of transit times considered in case b); (b) for a distribution of transit times. What we have found is that, for the baseline parameters and distribution of transit times of Fig. 1, OEF = 0.55 and OEF$_\text{mCTT}$ = 0.52, where OEF and OEF$_\text{mCTT}$ are the oxygen extraction factor in the single and multiple transit time cases, respectively. For the case of Fig. 2, we have found OEF = 0.67 and OEF$_\text{mCTT}$ = 0.54. These results are in qualitative agreement with those reported by Jespersen and Østergaard,[17] showing a lower oxygen extraction factor in the case of multiple versus single capillary transit times.

For the calculations of the average capillary and venous saturations we have derived the capillary blood flow velocity and capillary length distributions from the distribution of capillary transit times. For this purpose we have used Poiseuille's law for the resistance of a blood vessel and a simple circuital equivalent relationship between the pressure difference at the extremities of the blood vessel and the blood flow in the vessel. Calculations of the average capillary and venous saturations have shown that for capillary transit time distributions characterized by $\sigma(\tau)/\langle\tau\rangle \lesssim 80\%$, the average capillary saturation is always greater than the average venous saturation, but the opposite is true for wider distributions.

For the results of this work we have assumed no change in oxygen metabolic rate. This is only an approximation, since if α (the net rate of oxygen transfer from blood to tissue) does not change (as we have assumed), the cerebral metabolic rate of oxygen oscillates in phase with cerebral blood flow. More precisely, the relationship between cerebral blood flow oscillations (**cbf**) and cerebral metabolic rate of oxygen oscillations (**cmro$_2$**) for α fixed is[25]: **cmro$_2$** = **cbf**$(1 - \frac{S^{(v)}}{\langle S^{(c)} \rangle})$. We note that in this case the changes in oxygen consumption are only induced by flow oscillations (and associated oscillations in the oxygen concentration in capillary blood) and their average value over a period is zero (which is not the case during a period of brain activation that is associated with an increased cerebral metabolic demand). Given the fact that, in the model equations, **cbf** and **cmro$_2$** only appear combined in their difference [**cbf**(ω) − **cmro$_2$**(ω)], the above observations lead to the conclusion that an in-phase contribution from **cmro$_2$**(ω) has an effect that is equivalent to a reduction in **cbf**(ω).

Given the autoregulation high pass relationship between volume and flow oscillations [Eq. (8)], we can show that a reduction of cbf(ω) amplitude will not affect the CHS spectra as long as equal arterial and venous volume oscillations are considered.[12]

In addition to a single capillary transit time, the original model also considers a single venous transit time, thus assuming that microvascular hemodynamics can be represented by effective transit times instead of the actual distribution of blood transit times. We have run some additional calculations to study the dependence of CHS spectra on the distribution of venous blood transit times by also using a gamma distribution with $\langle t^{(v)} \rangle = 3$ s and $\sigma(t^{(v)}) = 1.22$ s. We have found that the distribution of venous transit times has a more negligible effect on the calculated CHS spectra than the distribution of capillary transit times.

5. Conclusions and Future Directions

In this work, we have compared the spectra calculated in CHS by using two models: (a) our original model which considers effective, single-valued capillary and venous transit times to describe the entire microvasculature; (b) an extended model which considers a distribution of capillary transit times for the calculation of CHS spectra. We have found that our original model can reproduce the spectra obtained with the extended model (to within typical experimental errors) for distributions having

standard deviation $[\sigma(\tau)]$ and mean value $(\langle\tau\rangle)$ verifying $\sigma(\tau)/\langle\tau\rangle \lesssim 45\%$. Future work will further quantify the difference between the original and extended models in terms of the values of the six physiological parameters that are obtained by fitting the measured CHS spectra.[12] More specifically, we will generate CHS spectra with the extended model, assign random errors to the data points, and run the inverse procedure based on a fit with our original model (considering only a single capillary transit time). In this fashion, we will quantify the errors on the recovered physiological parameters associated with the approximation of distributions of capillary and venous blood transit times with single, effective values.

Another future direction of our work will be concerned with the robustness of our results when different distribution functions are chosen. In fact, the gamma distribution used here and previously proposed[17] does not always closely match experimentally measured capillary transit time distributions.[23]

Finally, the fact that in our calculations we have neglected changes in the metabolic rate of oxygen $[\mathbf{cmro_2}(\omega) = 0]$ means that this study is applicable to cases where the high-pass filter relationship between flow and volume is the relevant one, and the effects of oxygen consumption changes on the CHS spectra can be neglected, as we have argued in the discussion. We plan on further exploring whether cases in which changes in metabolic rate of oxygen may not be neglected (such as functional brain studies) require additional considerations and determine new results.

Acknowledgments

References

1. S. Fantini, "Dynamic model for the tissue concentration and oxygen saturation of hemoglobin in relation to blood volume, flow velocity, and oxygen consumption: Implications for functional neuroimaging and coherent hemodynamics spectroscopy (CHS)," *Neuroimage* **85**, 202–221 (2014).
2. R. B. Buxton, "Dynamic models of BOLD contrast", *Neuroimage* **62**, 953–961 (2012).
3. Y. Zheng, D. Johnston, J. Berwick, D. Chen, "A three compartment model of the hemodynamic response and oxygen delivery to brain," *Neuroimage* **28**, 925–939 (2005).
4. S. G. Diamond, K. L. Perdue, D. A. Boas, "A cerebrovascular response model for functional neuroimaging including dynamic cerebral autoregulation," *Math. Biosci.* **220**, 102–117 (2009).
5. T. J. Huppert, M. S. Allen, S. G. Diamond, D. A. Boas, "Estimating cerebral oxygen metabolism from fMRI with a dynamic mulitcompartment windkessel model," *Hum. Brain Mapp.* **30**, 1548–1567 (2009).
6. L. Kocsis, P. Herman, A. Eke, "Mathematical model for the estimation of hemodynamic and oxygenation variables by tissue spectroscopy," *J. Theor. Biol.* **241**, 262–275 (2006).
7. S. Fantini, "A hemodynamic model for the physiological interpretation of *in vivo* measurements of the concentration and oxygen saturation of hemoglobin," *Phys. Med. Biol.* **47**, N249–N257 (2002).
8. D. A. Boas, S. R. Jones, A. Devor, T. J. Huppert, A. M. Dale, "A vascular anatomical network model of the spatio-temporal response to brain activation," *Neuroimage* **40**, 1116–1129 (2008).
9. F. Hyder, R. G. Shulman, D. L. Rothman, "A model for the regulation of cerebral oxygen delivery," *J. Appl. Physiol.* **85**, 554–564 (1998).
10. M. L. Pierro, B. Hallacoglu, A. Sassaroli, J. M. Kainerstorfer, S. Fantini, "Validation of a novel hemodynamic model for coherent hemodynamics spectroscopy (CHS) and functional brain studies with fNIRS and fMRI," *Neuroimage* **85**, 222–233 (2014).
11. M. L. Pierro, J. M. Kainerstorfer, A. Civiletto, D. E. Weiner, A. Sassaroli, B. Hallacoglu, S. Fantini, "Reduced speed of microvascular blood flow in hemodialysis patients versus healthy controls: A coherent hemodynamics spectroscopy study," *J. Biomed. Opt.* **19**, 026005 1–9 (2014).
12. J. M. Kainerstorfer, A. Sassaroli, B. Hallacoglu, M. L. Pierro, S. Fantini, "Practical steps for applying a new dynamic model to near-infrared spectroscopy measurements of hemodynamic oscillations and transient changes: Implications for cerebrovascular and functional brain studies," *Acad. Radiol.* **21**, 185 (2014).
13. J. L. Chen, L. Wei, V. Acuff, D. Bereczki, F. J. Hans, T. Otsuka, W. Finnegan, C. Patlak, J. Fenstermacher, "Slightly altered permeability-surface area products imply some cerebral capillary recruitment during hypercapnia," *Microvasc. Res.* **48**, 190–211 (1994).
14. U. Gobel, B. Klein, H. Schrock, W. Kuschinsky, "Lack of capillary recruitment in the brains of

awake rats during hypercapnia," *J. Cereb. Blood Flow Metab.* **9**, 491–499 (1989).

15. R. R. Diehl, D. Linden, D. Lucke, P. Berlit, "Phase relationship between cerebral blood-flow velocity and blood-pressure — a clinical-test of auto-regulation," *Stroke* **26**, 1801–1804 (1995).

16. A. P. Blaber, R. L. Bondar, F. Stein, P. T. Dunphy, P. Moradshahi, M. S. Kassam, R. Freeman, "Transfer function analysis of cerebral autoregula-tion dynamics in autonomic failure patients," *Stroke* **28**, 1686–1692 (1997).

17. S. N. Jespersen, L. Østergaard, "The roles of cere-bral blood flow, capillary transit time heterogeneity, and oxygen tension in brain oxygenation and metabolism," *J. Cereb. Blood Flow Metab.* **32**, 264–277 (2012).

18. F. Cassot, F. Lauwers, C. Fouard, S. Prohaska, V. Lauwers-Cances, "A novel three dimensional computer-assisted method for a quantitative study of microvascular networks of the human cerebral cortex," *Microcirculation* **13**, 1–18 (2006).

19. A. R. Pries, T. W. Secomb, *Handbook of Physiology: Microcirculation*, Academic press, San Diego (2008).

20. R. L. Grubb, M. E. Raichle, J. O. Eichling, M. M. Ter-Pogossian, "The effects of changes in $PaCO_2$ on cerebral blood volume, blood flow, and vascular mean transit time," *Stroke* **5**, 630–639 (1974).

21. I. Kida, D. L. Rothman, F. Hyder, "Dynamics of changes in blood flow, volume, and oxygenation: Implications for dynamic functional magnetic reso-nance imaging calibration," *J. Cereb. Blood Flow Metab.* **27**, 690–696 (2007).

22. D. Kleinfeld, P. P. Mitra, F. Helmchen, W. Denk, "Fluctuations and stimulus-induced changes in blood flow observed in individual capillaries in layers 2 through 4 of rat neocortex," *Proc. Natl. Acad. Sci.* **95**, 15741–15746 (1998).

23. B. Stefanovic, E. Hutchinson, V. Yakovleva, V. Schram, J. T. Russell, L. Belluscio, A. P. Koretsky, A. C. Silva, "Functional reactivity of cerebral capillaries," *J. Cereb. Blood Flow Metab.* **28**, 961–972 (2008).

24. S. Sakadžic, E. T. Mandeville, L. Gagnon, J. J. Musacchia, M. A. Yaseen, M. A. Yucel, J. Lefebvre, F. Lesage, A. M. Dale, K. Eikermann-Haerter, C. Ayata, V. J. Srinivasan, E. H. Lo, A. Devor, D. A. Boas, "Capillary oxygenation is lower than venous because of capillary transit time heterogeneity," *Proceedings of the 42nd Conference of the Interna-tional Society on Oxygen Transport in Tissue (Isott)*, London, UK, 28 June–3 July 118 (2014), p. 118.

25. S. Fantini, "A new hemodynamic model shows that temporal perturbations of cerebral blood flow and metabolic rate of oxygen cannot be measured indi-vidually using functional near-infrared spectro-scopy," *Physiol. Meas.* **35**, N1–N9 (2014).